Refractory, Ceramic, and Composite Materials
Тугоплавкие, керамические и композиционные материалы

UDC 546.271
https://doi.org/10.17073/1997-308X-2023-2-35-45

Research article
Научная статья

Synthesis of B_4C–TiB_2 composition powder mixtures by carbidobor reduction using nanofibrous carbon for ceramic fabrication

T. S. Gudyma[1], Yu. L. Krutskii[1], E. A. Maksimovskiy[2], N. Yu. Cherkasova[1], N. I. Lapekin[1], T. V. Larina[3]

[1] **Novosibirsk State Technical University**
20 Karl Marks Prosp., Novosibirsk 630073, Russia
[2] **Nikolaev Institute of Inorganic Chemistry, Siberian Branch of the Russian Academy of Sciences**
3 Lavrent'eva Prosp., Novosibirsk 630090, Russia
[3] **Boreskov Institute of Catalysis, Siberian Branch of the Russian Academy of Sciences**
5 Lavrent'eva Prosp., Novosibirsk 630090, Russia

gudymatan@mail.ru

Abstract. The results of the researching process of obtaining composition powder material B_4C–TiB_2 by carbide reduction of titanium dioxide, using carbon reducing agent – carbon nanofibers, are presented. Furthermore, the results of studying of some properties of ceramics made using the synthesized powder are presented. The synthesis of composite materials was carried out in an induction crucible furnace for 20 min in the temperature range of 1200–1900 °C in an argon atmosphere. It has been established that the optimum temperature of the synthesis is 1650 °C, irrespective of the batch composition. The characteristics of the composite powders containing 10–30 mol. % of the TiB_2 phase have been studied. *X*-ray electron microscopy has revealed that the particles of the powder are predominantly aggregated. There are two peaks in the particle size distribution histograms. The part of the histogram with a smaller particle size mainly characterizes the B_4C phase. The part of the histogram with a larger particle size characterizes the TiB_2 phase. The average particle size of the B_4C phase is in the range of 5.3–5.5 μm, and that of the TiB_2 phase is in the range of 33.6–41.9 μm. The average size of 50 % of composite powder's particles for these contents does not exceed 13.4 μm. The surface area of the samples does not exceed 5 m^2/g. The oxidation of the composite powder materials by atmospheric oxygen begins at a temperature of approximately 500 °C. At the same time, when the temperature reaches 1000 °C, no more than 45 wt. % of the studied powders is oxidized. Ceramics made with the synthesized powder mixture B_4C + 30 mol. % TiB_2 by hot pressing has shown rather high values of relative density (99.0±1.1 %) and fracture toughness (5.0±0.2 $MPa \cdot m^{0.5}$).

Keywords: boron carbide, titanium diboride, carbide reduction, nanofibrous carbon (NFC), high-temperature synthesis

Acknowledgements: The research was performed in accordance with the state order of the Ministry of Education and Science (code FSUN-2023-0008).

For citation: Gudyma T.S., Krutskii Yu.L., Maksimovskiy E.A., Cherkasova N.Yu., Lapekin N.I., Larina T.V. Synthesis of B_4C–TiB_2 composition powder mixtures by carbidobor reduction using nanofibrous carbon for ceramic fabrication. *Powder Metallurgy and Functional Coatings*. 2023;17(2):35–45. https://doi.org/10.17073/1997-308X-2023-2-35-45

Синтез композиционных порошковых смесей B_4C–TiB_2 методом карбидоборного восстановления с использованием нановолокнистого углерода для изготовления керамики

Т. С. Гудыма[1], Ю. Л. Крутский[1], Е. А. Максимовский[2], Н. Ю. Черкасова[1], Н. И. Лапекин[1], Т. В. Ларина[3]

[1] **Новосибирский государственный технический университет**
630073, г. Новосибирск, пр-т Карла Маркса, 20
[2] **Институт неорганической химии им. А.В. Николаева Сибирского отделения РАН**
630090, г. Новосибирск, пр-т Академика Лаврентьева, 3
[3] **Институт катализа им. Г.К. Борескова Сибирского отделения РАН**
630090, г. Новосибирск, пр-т Академика Лаврентьева, 5

gudymatan@mail.ru

Аннотация. Представлены результаты исследования процесса получения порошковых смесей B_4C–TiB_2 методом карбидоборного восстановления диоксида титана в присутствии восстановителя – нановолокнистого углерода, а также изучения некоторых свойств керамики, изготовленной с использованием синтезированного порошка. Синтез порошковых смесей проводили в индукционной тигельной печи в течение 20 мин в диапазоне температур 1200–1900 °С в среде инертного газа – аргона. Установлено, что оптимальная температура процесса синтеза независимо от состава шихты составляет 1650 °С. Изучены характеристики порошков, содержащих 10–30 мол. % фазы TiB_2. Методом рентгеновской электронной микроскопии установлено, что частицы порошка преимущественно агрегированы. На гистограммах распределения частиц по размерам присутствуют два пика: первый (с меньшим размером частиц) в основном характеризует фазу B_4C, а второй (с крупными частицами) – фазу TiB_2. Средний размер частиц фазы B_4C составляет 5,3–5,5 мкм, а фазы TiB_2 – 33,6–41,9 мкм. Средний размер 50 % частиц порошка для исследуемых составов не больше 13,4 мкм. Величина удельной поверхности образцов не превышает 5 $м^2/г$. Окисление полученных смесей кислородом воздуха начинается при температуре около 500 °С. При этом при достижении температуры 1000 °С окисляется не более 45 мас. % исследуемых порошков. Керамика, изготовленная с использованием синтезированной порошковой смеси B_4C + 30 мол. % TiB_2 методом горячего прессования, продемонстрировала достаточно высокие значения относительной плотности (99,0±1,1 %) и трещиностойкости (5,0±0,2 $МПа·м^{0,5}$).

Ключевые слова: карбид бора, диборид титана, карбидоборное восстановление, нановолокнистый углерод (НВУ), высокотемпературный синтез

Благодарности: Исследование выполнено в соответствии с госзаданием Минобрнауки (код FSUN-2023-0008).

Для цитирования: Гудыма Т.С., Крутский Ю.Л., Максимовский Е.А., Черкасова Н.Ю., Лапекин Н.И., Ларина Т.В. Синтез композиционных порошковых смесей B_4C–TiB_2 методом карбидоборного восстановления с использованием нановолокнистого углерода для изготовления керамики. *Известия вузов. Порошковая металлургия и функциональные покрытия*. 2023;17(2):35–45. https://doi.org/10.17073/1997-308X-2023-2-35-45

Introduction

Over the past 20 years, the study of the production and properties of B_4C–TiB_2 composite ceramics has attracted a great interest, driven by the combination of the unique properties of their components – boron carbide and titanium diboride.

Boron carbide exhibit a high melting temperature (2447 °C) and possesses a unique combination of high hardness (up to 43 GPa) and low density (2.52 g/cm^3) [1; 2]. However, ceramics based on it are characterized by poor sintering and low fracture toughness. The use of modifying additives, such as titanium diboride, can significantly increase these indices by 10–40 % [3; 4].

Titanium diboride, as well as boron carbide, is a refractory compound, its melting temperature is ~3225 °C [5]. The microhardness of TiB_2 ceramics is rather high and amounts to 25–35 GPa. Titanium diboride exhibit a relatively high thermal conductivity coefficient (66.4 W/(m·K)) and low specific electrical toughness (~10^{-7} Ohm·m) [6; 7]. Furthermore, TiB_2 is quite stable when heated in air, and it is not oxidized at a temperature

of up to 800 °C. At a temperature of 900 °C, it is slightly oxidized with the formation of a vitreous protective film on the surface of the material, which prevents its further oxidation [8].

Many researchers note an increase in the fracture toughness and sinterability of the ceramics based on B_4C–TiB_2 system in comparison with the ceramics containing only B_4C [9; 10]. The presence of TiB_2 prevents the growth of B_4C grains, reduces the sintering temperature and improves the mechanical properties of the resulting composite [11; 12]. Besides, there are data [13; 14] being indicative of the fact that the presence of TiB_2 increases the electrical conductivity of B_4C–TiB_2 material. B_4C–TiB_2 composite of eutectic composition can itself act as a modifying additive for refractory ceramics, increasing its mechanical properties [15].

In most cases, ready-made B_4C and TiB_2 powders are used as batch components for the production of B_4C–TiB_2 composite ceramic material [14; 16]. The preparation of such a batch before compaction involves mixing using a planetary ball mill.

The literary sources present the data on the production of B_4C–TiB_2 composites by *in situ* methods in accordance with reactions (1) [17], (2) [3] and (3) [18]:

$$Ti + 6B + C = B_4C + TiB_2, \quad (1)$$

$$TiC + 6B = B_4C + TiB_2, \quad (2)$$

$$(1 + x)B_4C + 2xTiO_2 + 3xC = \\ = B_4C + 2xTiB_2 + 4xCO. \quad (3)$$

The advantage of running the processes in accordance with reactions (1) and (2) is the absence of gaseous products, which is particularly important for the simultaneous synthesis and compaction of the material. On the other hand, the use of expensive boron and long-term mixing of the batch are required. Reaction (3) is prospective for the preliminary production of B_4C–TiB_2 batch due to the use of cheaper reagents. For instance, in terms of producing a mixture with a molar ratio of B_4C:TiB_2 = 1:1, the cost of reagents for reaction (3) is almost 5 times lower than for reactions (1) and (2). In addition, the gaseous product release during the heat treatment can contribute to additional mixing of the batch and more uniform heating.

Acetylene black is most often used as a carbon source in carbide synthesis. This material exhibit a rather high surface area of ~50 m^2/g. However, nanofibrous carbon (NFC) with a developed surface area (~150 m^2/g) can serve as a more efficient carbon material [19]. A highly dispersed carbon agent can accelerate the formation of titanium diboride due to more intensive diffusion of carbon into titanium dioxide particles. It should be noted that there are some technological challenges in using NFC. This highly dispersed material is prone to caking and requires thorough homogenization of the reaction mixture before the heat treatment. Besides, NFC is a more expensive reagent, its price is about 5 times higher than that of acetylene black. However, in light of the fact that the mass fraction of carbon agent in the reaction mixture for reaction (3) is relatively low, the cost of final product increases insignificantly.

The purpose of this paper is to research the synthesis and study the properties of $B_4C + TiB_2$ composite powder materials obtained by the carbide reduction of titanium dioxide (reaction (3)) using NFC.

Research methods

To obtain $B_4C + TiB_2$ powder composites, the following reagents were used:

– highly dispersed boron carbide B_4C (assay 98.5 wt. %, average particle size d = 2.1 μm) synthesized from simple substances according to method [20];

– titanium dioxide (TU 6-09-3811-79, assay 99.0 wt. %, d = 1.0 μm);

– nanofibrous carbon (carbon content 99 wt. %) [21; 22].

The used NFC contained catalyst residues: ~0.1 wt. % Al_2O_3 and 0.9 wt. % Ni. In its initial form, the carbon material consisted of pellets being 0.4–8.0 mm in size formed by densely intertwined fibers with an average diameter of 73 nm. The NFC pellets were pre-ground in the AGO-2S planetary ball mill for 5 min at an acceleration of 15g and a NFC to ball mass ratio of 1:15. The average particle size of NFC after grinding was 3.9 μm.

According to the diagram of B_4C–TiB_2 system state at the eutectic point, the content of TiB_2 is ~26 mol. % [23]. The composite powder materials, the composition of which corresponds to the eutectic point and beyond it, were selected for research. The ratio of reagents was selected so that the composite powder materials containing 10, 20, 25, and 30 mol. % of TiB_2 were obtained in accordance with reaction (3). In calculating the batch composition, the presence of impurities in the composition of reagents was taken into account. The samples were designated as T10, T20, T25 and T30, respectively. The initial powders were mixed in a planetary ball mill for 5 min at an acceleration of 20g, and then they were sifted through a sieve with a mesh size of 100 μm.

The synthesis was performed in the VCh-25AV induction crucible furnace (Russia). Argon was chosen as an inert atmosphere preventing nitriding of boron

carbide and titanium diboride. During carbide reduction of titanium dioxide, gaseous products (CO and CO_2) are released and the pressure in the system increases. To ensure the safety of the process, the synthesis should be performed in a flow reactor, ensuring continuous removal of the resulting gases by an argon flow. The temperature was controlled using the Kelvin Compact 2300 optical pyrometer (PC EUROMIX, Russia). The pressure in the reactor was almost atmospheric. The temperatures of the beginning of titanium dioxide reduction were determined by performing the thermodynamic calculations in accordance with the procedure [24]. The temperatures were calculated for different CO pressures, since it is difficult to estimate the partial pressure of CO in Ar + CO gas mixture.

The value of the isobaric-isothermal potential of the reaction of carbide reduction of titanium dioxide turns negative at the temperatures of 745, 849 and 994 °C for CO pressures of 0.001, 0.01 and 0.1 MPa, respectively.

In this research, the heat treatment of the batch was initially performed to prepare a mixture of B_4C–25 mol. % TiB_2 (T25) at $t = 1200$, 1400, 1650 and 1900 °C for 20 min in accordance with reaction (3). The completeness of the process was evaluated by weighing the batch and the reaction products, as well as by comparing experimental data with the theoretical ones. The estimated weight loss upon the completeness of this reaction was 19.05 wt. %. In practice, this value may slightly differ from the estimated value. This is due to the presence of impurities in the reagents used, as well as due to the possibility of the formation of aluminum borocarbide $Al_3B_{48}C_2$, being prone to oxidation and hydration, during the synthesis. Since the results of the conducted studies revealed that the optimal synthesis temperature is 1650 °C, further experiments with a batch of a different composition were performed at the same temperature for 20 min.

The *X*-ray phase analysis (XPA) of the obtained powders was performed by means of DRON-3 diffractometer using CuK_α-radiation. The diffraction patterns were interpreted using Power Diffraction File (PDF-2) database. The ratio of B_4C and TiB_2 phases was estimated using the corundum number method.

The total carbon content was determined by infrared absorption spectrometry using the CS 844 sulfur and carbon analyzer (LECO Corporation, the USA) as per GOST 12344-2003.

The microstructure of the powders and the morphology of the particles were studied using S-3400N scanning electron microscope (Hitachi, Japan) equipped with an energy-dispersive analysis attachment (Oxford Instruments Analytical, the United Kingdom). The particle size distribution was evaluated by means of laser particle size analyzer MicroSizer 201 VA Instrument (VA Instalt LLC, Russia). The surface area was determined by the method of low-temperature nitrogen adsorption using NOVA 2200e device (Quantachrome Instruments, the USA).

The thermal-oxidative stability of the samples was determined using STA 449 C Jupiter synchronous thermal analysis instrument (Netzsch, Germany). During the analysis, the sample was oxidized in an atmosphere of synthetic air when heated up to a temperature of 1000 °C at a rate of 15 °C/min.

Experiments on the production of B_4C–TiB_2 composite ceramics were performed on a hot pressing unit designed by the Institute of Automation and Electrometry, the Siberian Branch of the Russian Academy of Sciences (Novosibirsk), using a synthesized powder containing 30 mol. % of TiB_2. In this case, the batch was pre-ground in a planetary ball mill at an acceleration of 20*g* for 5 min at a mass ratio of the batch to balls of 1:30. The process was carried out in argon atmosphere at a pressing pressure of 25 MPa and a temperature of 2100 °C.

The relative density and open porosity of ceramics were evaluated in accordance with GOST 2409-2014 using AD-1653 hydrostatic weighing set installed on GR-300 analytical balance (AND, Japan).

Vickers microhardness measurements were performed on 402MVD unit (Wolpert Group, Great Britain). The indentation load was 500 g. At least 5 punctures were applied to the samples in such a way that the distance between the center of one indent and the edge of the next one was at least 2.5 lengths of the diagonal of the indent.

The fracture toughness was determined by indentation on a hardness tester of TP model No. 3534 (Russia) with an indenter in the form of a 4-sided diamond Vickers pyramid with a load of 5 kg. Its values were calculated according to equation [25]

$$K_{1c} = 0.048\left(\frac{l}{a}\right)^{-0,5}\left(\frac{H_v}{E\Phi}\right)^{-0,4}\frac{H_v a^{0,5}}{\Phi},$$

where l is the fracture length, μm; a is the half-diagonal of impression, μm; H_v is the microhardness, GPa; E is the Young modulus, GPa; $\Phi = 3$ is the constant.

Results and discussion

Fig. 1 shows the *X*-ray diffraction patterns of the synthesized samples of B_4C–25 mol. % TiB_2 mixture. It can be seen that at the synthesis temperatures $t = 1200$ and 1400 °C the peaks of both the target B_4C and TiB_2 phases and the unreacted carbon are observed for condensed products. At $t = 1650$ and 1900 °C, B_4C and TiB_2 phases are formed in the reaction products, and the *X*-ray diffraction patterns show the impurity reflections of $Al_3B_{48}C_2$

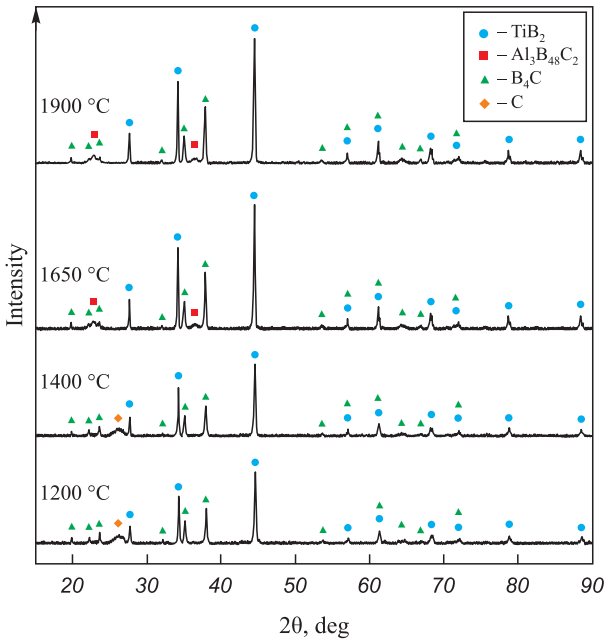

Fig. 1. The diffraction patterns of the samples of B_4C–25 mol. % TiB_2 mixtures obtained at the temperatures of 1200–1900 °C

Рис. 1. Дифрактограммы образцов смесей B_4C–25 мол. % TiB_2, полученных при температурах 1200–1900 °C

phase. Its presence is caused by the fact that NFC has aluminum oxide impurity Al_2O_3, which reacts with the components of the batch [20].

Fig. 2 presents the electron micrographs of mixture samples synthesized at the temperatures of 1400, 1650 and 1900 °C. The micrographs were taken in the mode of registration of secondary electrons. The scanning electron microscopy (SEM) images of a sample obtained at $t = 1400$ °C clearly show heterogeneous particles, some of which are fragmented. To clarify their nature, an elemental mapping was performed, which indicated that the particles constituted remains of unreacted NFC (Fig. 3). Besides, the energy- dispersive analysis data revealed the presence of oxygen in the amount of 5 wt. %.

The samples obtained at $t = 1650$ and 1900 °C have aggregated particles with smooth edges, the size of which does not exceed several micrometers. According to the energy-dispersive analysis, these samples contain titanium, boron, carbon, as well as nickel and aluminium (~1 wt. % in total).

The theoretical weight loss of the batch as a result of reaction (3) is 19.05 % at a ratio of reagents corresponding to 25 mol. % of TiB_2 in the resulting powder. The experimental weight loss was 0.9, 1.7, 19.5 and 19.4 % at the processing temperatures of 1200, 1400, 1650 and 1900 °C, respectively. It follows from the obtained results that the reaction of boride formation is fully completed at $t = 1650$ °C.

The results of granulometric analysis of the samples of B_4C –25 mol. % TiB_2 composition synthesized at $t = 1650$ and 1900 °C showed that the average particle size of the obtained powders increases from 8.4 to 9.8 μm upon an increase in the synthesis temperature. Since an increase in the particle size of the powder can lead to adeterioration in its sintering properties, the further experiments at $t = 1650$ °C were conducted.

To evaluate the effect of the mixture composition on the properties of the resulting powder, the batch with the composition corresponding to 10, 20, 25 and

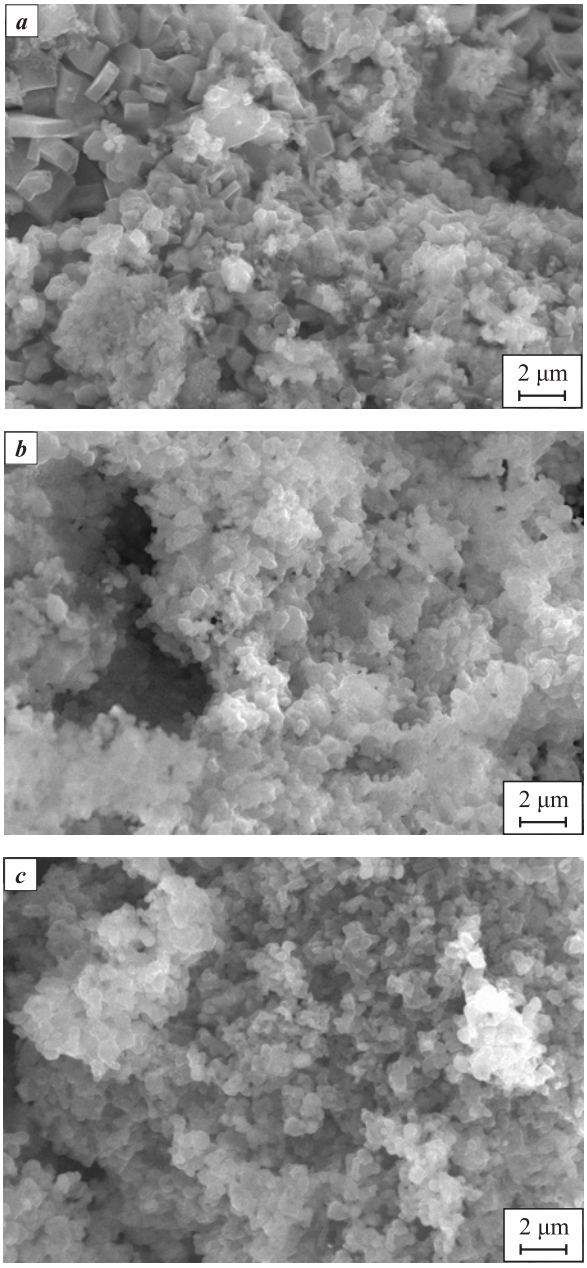

Fig. 2. The SEM images of B_4C–TiB_2 powders synthesized at $t = 1400$ °C (***a***), 1650 °C (***b***) and 1900 °C (***c***)

Рис. 2. Снимки РЭМ порошков B_4C–TiB_2, синтезированных при $t = 1400$ °C (***a***), 1650 °C (***b***) и 1900 °C (***c***)

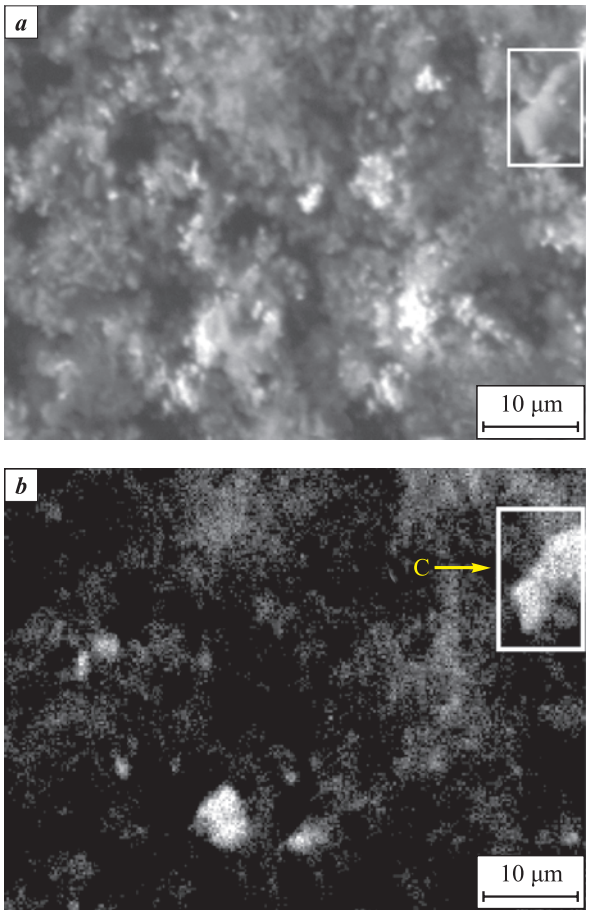

Fig. 3. The micrograph of B_4C–TiB_2 powder synthesized at t = 1400 °C (***a***), and the distribution of carbon (***b***)

Рис. 3. Микрофотография порошка B_4C–TiB_2, синтезированного при t = 1400 °C (***a***), и распределение углерода (***b***)

30 mol. % of TiB_2 was heat-treated. The experimental weight loss of the batch during the synthesis was close to the theoretical value in all cases (the relative deviation did not exceed 3 %), which indicates the completeness of the synthesis process at t = 1650 °C, regardless of the composition of the sample. This was also confirmed by *X*-ray phase analysis data (Fig. 4). The diffraction patterns of the condensed reaction products contain TiB_2 and B_4C phases for all samples. The TiB_2 phase content estimated by the corundum number method was 9, 18, 24, and 29 mol. % for T10, T20, T25, and T30 samples, respectively. These data turned out to be close to the estimated values.

From the results of determining the total carbon content, presented in Table 1, it can be seen that the obtained experimental data slightly exceed the values corresponding to the given composition of the synthesized mixtures. This also indicates a complete synthesis process. It should be noted that with an increase in TiB_2 phase content in the powders, the excess of carbon decreases.

Fig. 5 shows the micrographs of the samples of composite powder materials with different TiB_2 contents. All SEM images contain aggregated particles of several micrometers in size, and the absence of fragmented particles indirectly bespeaks of the absence of unreacted particles of the initial components of the reaction mixture.

In the course of particle size analysis, the samples of B_4C–TiB_2 powders were subjected to ultrasonic dispersion at a power of 200 W for 30 s. Two peaks were found in the particle size distribution histograms of T10 and T30 samples (Fig. 6), with the second peak increasing upon an increase in TiB_2 phase content. Since the ratio of the heights of the first and the second maxima on the bimodal curve changes with an increase in the concentration of titanium diboride in the synthesized mixture, it can be assumed

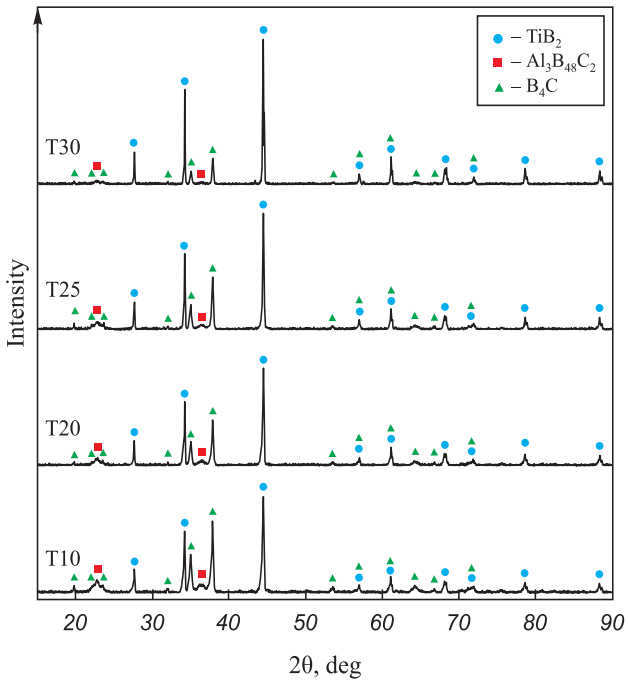

Fig. 4. The diffraction patterns of the samples of powder mixtures containing 10–30 mol. % TiB_2, synthesized at t = 1650 °C

Рис. 4. Дифрактограммы образцов порошковых смесей, содержащих 10–30 мол. % TiB_2, синтезированных при t = 1650 °C

Table 1. **The results of determining the total carbon content, wt. %**

Таблица 1. **Результаты определения содержания общего углерода, мас. %**

Sample	Experiment	Calculation
T10	19.7	19.1
T20	16.8	16.5
T25	15.4	15.3
T30	14.2	14.1

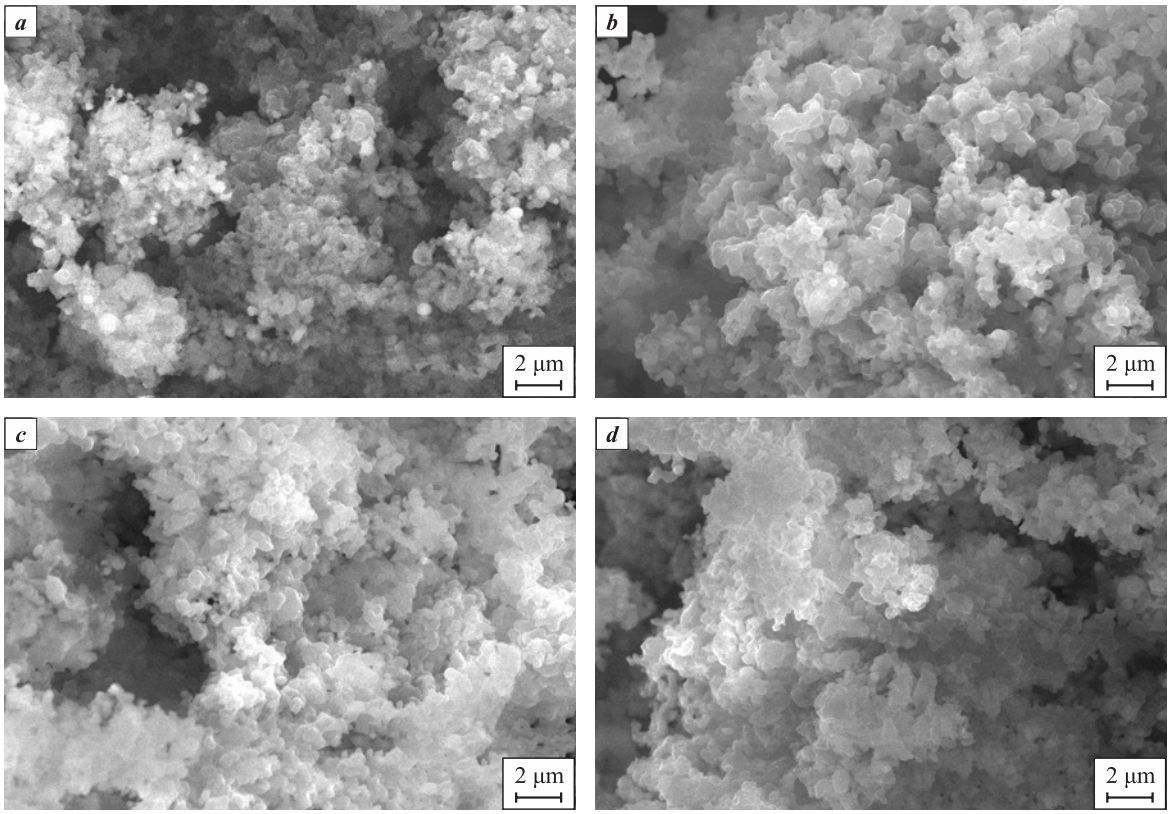

Fig. 5. The micrographs of B_4C–TiB_2 powder synthesized at t = 1650 °C
TiB_2 content, mol. %: 10 (***a***), 20 (***b***), 25 (***c***) and 30 (***d***)

Рис. 5. Микрофотографии образцов порошковых смесей B_4C–TiB_2, синтезированных при t = 1650 °C
Содержание TiB_2, мол. %: 10 (***a***), 20 (***b***), 25 (***c***) и 30 (***d***)

that the part of the histogram with a smaller particle size mainly characterizes the B_4C phase; consequently, its other part with a larger particle size refers to the TiB_2 phase. Based on this assumption, the average size of particles and aggregates was calculated for each phase (Table 2), and the values of standard deviations and asymmetry indices were determined using method [26].

Table 2 shows that the average 50 % particle size increases with an increase in the TiB_2 content of the powders under research. There is also an increase in the particle size of B_4C phase compared to pure B_4C (2.4 μm). The standard deviation values indicate a wide range in particle size distribution, i.e. the powder is polydisperse. The low value of asymmetry degree proves the symmetry of the distribution curves for each phase. The largest value of the average particle size of B_4C and TiB_2 phases is typical for the sample containing 30 mol. % of TiB_2.

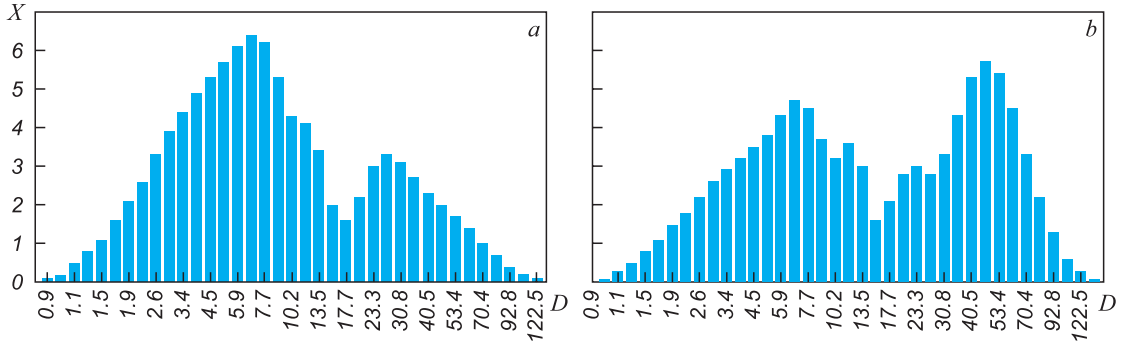

Fig. 6. Particle size distribution histograms for T10 (***a***) and T30 (***b***) samples
X – fraction content, wt. %; *D* – particle size, μm

Рис. 6. Гистограммы распределения частиц по размерам образцов T10 (***a***) и T30 (***b***)
X – содержание фракции, мас. %; *D* – размер частиц, мкм

Table 2. **The results of research of particle size of B_4C–TiB_2 powders**

Таблица 2. **Результаты исследования размера частиц порошков B_4C–TiB_2**

Sample	Average size of 50 % of particles D50, μm	Phase	Average size of the phase, μm	Standard deviation, μm	Asymmetry degree
T10	7.4	B_4C	5.3	1.9	–0.050
		TiB_2	33.6	1.6	0.040
T20	8.3	B_4C	5.0	1.9	–0.040
		TiB_2	40.0	1.6	0.010
T25	8.4	B_4C	5.1	1.9	–0.040
		TiB_2	41.0	1.6	–0.023
T30	13.4	B_4C	5.5	1.9	–0.050
		TiB_2	41.9	1.6	–0.005

The surface area values were 5, 4, 3, and 3 m^2/g for T10, T20, T25, and T30 samples, respectively, whereas the said value was 4 m^2/g for the initial boron carbide sample without modifying additives.

In order to determine the thermal-oxidative stability of the obtained B_4C–TiB_2 powders, they were oxidized in a synthetic air atmosphere. Similar thermogravimetric curves were obtained for all samples of different composition. The derivatogram of T10 sample is presented in Fig. 7 as an example.

X-ray phase analysis was conducted to identify the products of oxidation of the mixture with oxygen. The diffraction pattern of the sample of composite powder material after heating up to 1000 °C in an oxidizing atmosphere is shown in Fig. 8.

The results of thermogravimetric analysis show that the weight gain is caused by the oxidation process starting at t ~500 °C. Upon the temperature reaching 1000 °C, there are unoxidized B_4C and TiB_2 phases, as well as $TiBO_3$, TiO_2 and B_2O_3 oxidation products present in the samples. It can be assumed that when this temperature is reached, the process proceeds in accordance with the following reactions

$$(1-x)B_4C + xTiB_2 + (3.5-0.25y)O_2 = (2-x-0.5y)B_2O_3 + (x-y)TiO_2 + yTiBO_3 + (1-x)CO, \quad (4)$$

$$(1-x)B_4C + xTiB_2 + (4-1.5x-0.25y)O_2 = (2-x-0.5y)B_2O_3 + (x-y)TiO_2 + yTiBO_3 + (1-x)CO_2. \quad (5)$$

Upon that, the oxidation of minimum 80 wt. % of composite powder material occurs. The mass fraction of the oxidized substances at t = 1000 °C is 80, 75, 69 and 73 wt. % for T10, T20, T25 and T30 samples, respectively, and 83 wt. % for the initial boron carbide. The incomplete oxidation of the samples can be

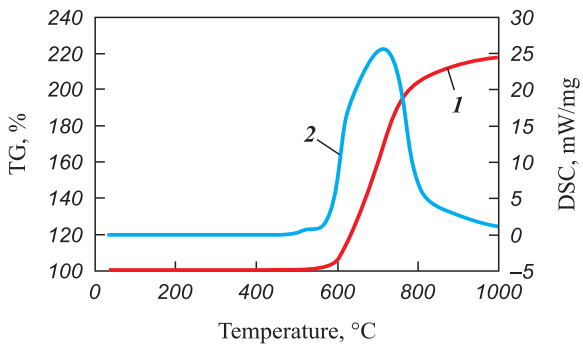

Fig. 7. TG (***1***) and DSC (***2***) curves for B_4C–10 mol. % TiB_2 (T10) sample

Рис. 7. Кривые ТГ (***1***) и ДСК (***2***) образца B_4C–10 мол. % TiB_2 (T10)

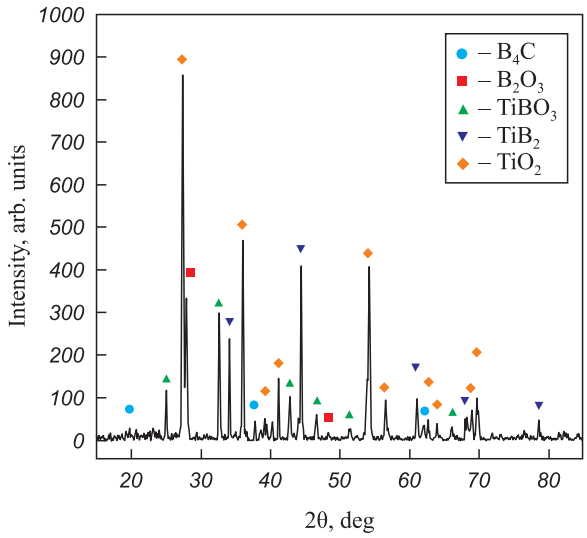

Fig. 8. The diffraction pattern of B_4C–25 mol. % TiB_2 (T25) sample subjected to oxidation in a synthetic oxygen atmosphere at t = 1000 °C

Рис. 8. Дифрактограмма образца B_4C–25 мол. % TiB_2 (T25), подвергнутого окислению в среде синтетического кислорода при t = 1000 °C

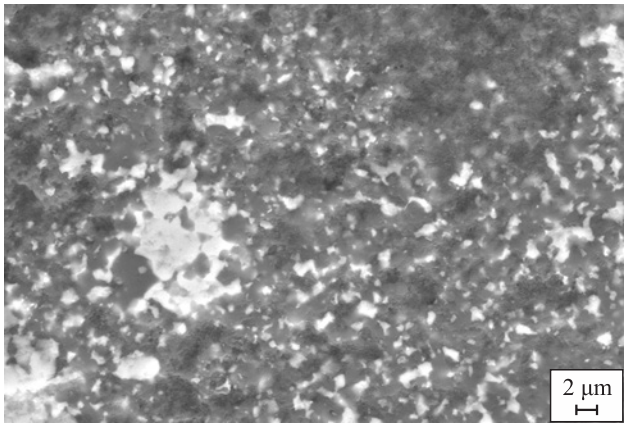

Fig. 9. The microstructure of B_4C–30 mol. % TiB_2 composite ceramics
Gray area – B_4C matrix, light inclusions – TiB_2

Рис. 9. Микроструктура композиционной керамики B_4C–30 мол. % TiB_2
Серые участки – матрица B_4C, светлые включения – TiB_2

explained by the formation of a liquid protective film of B_2O_3, the melting temperature of which is ~450 °C, on the surface of B_4C and TiB_2 particles [27].

The synthesized powder containing 30 mol. % of TiB_2 was selected for the preparation of composite ceramics. The relative density of the obtained material was 99.0±1.1 %, and the relative density of B^4C ceramics produced in a similar way without the use of modifying additives was 97.7±0.5 %.

Thus, the use of a batch with B_4C–30 mol. % TiB_2 composition obtained by carbide reduction allows to produce ceramics with a high relative density. Its structure consists of a boron carbide matrix (gray area) and light inclusions of titanium diboride of various sizes (Fig. 9).

The microhardness of the composite ceramics was 33.0±3.4 GPa, and the fracture toughness was 5.0±0.2 MPa·$m^{0.5}$; for ceramics without TiB_2 additives, these indices were 45.5±5.2 GPa and 3.6±0.11 MPa·$m^{0.5}$, respectively. Thus, the presence of a modifying additive in the composition of ceramics naturally led to a decrease in microhardness and an increase in the material fracture toughness.

Conclusion

B_4C–TiB_2 composite powder materials have been obtained by the carbide reduction of titanium dioxide using an excess of boron carbide and nanofibrous carbon. It has been established that the process of formation of the TiB_2 phase starts at t = 1200 °C, but it is fully completed at 1650 °C. a further increase in a temperature leads to an increase in the particle size of B_4C–TiB_2 powder. The average size of 50 % particles of the composite powder material containing 10–30 mol. % of TiB_2 is 15 μm maximum, and the surface area value does not exceed 5 m^2/g. The average particle size of the B_4C phase is in the range of 5.3–5.5 μm, and that of the TiB_2 phase is 33.6÷41.9 μm.

The oxidation of the obtained mixtures with atmospheric oxygen starts at t ~500 °C. Upon that, maximum 80 wt. % of the powders under study are oxidized when the temperature reaches 1000 °C.

The presence of 30 mol. % of TiB_2 in the composite powder material allows to perform the hot pressing production of the ceramics with a higher relative density (99.0±1.1 %) and fracture toughness (5.0±0.2 MPa·$m^{0.5}$) as compared to the ceramics obtained in a similar way only from B_4C.

References / Список литературы

1. Domnich V., Reynaud S., Haber R.A., Chhowalla M. Boron carbide: Structure, properties, and stability under stress. *Journal of the American Ceramic Society*. 2011;94(11):3605–3628. https://doi.org/10.1111/j.1551-2916.2011.04865.x
2. Krutskii Y.L., Nepochatov Y.K., Pel' A.N., Skovorodin I.N., Dyukova K.D., Krutskaya T.M., Kuchumova I.D., Mats O.E., Tyurin A.G., Emurlaeva Y.Y., Podryabinkin S.I. Synthesis of polydisperse boron carbide and synthesis of a ceramic on its basis. *Russian Journal of Applied Chemistry*. 2019;92(6):750–758. https://doi.org/10.1134/S1070427219060041

   Крутский Ю.Л., Непочатов Ю.К., Пель А.Н., Сковородин И.Н., Дюкова К.Д., Крутская Т.М., Кучумова И.Д., Матц О.Э., Тюрин А.Г., Эмурлаева Ю.Ю., Подрябинкин С.И. Синтез полидисперсного карбида бора и получение керамики на его основе. *Журнал прикладной химии*. 2019;92(6):719–727. https://doi.org/10.1134/S0044461819060045
3. Guo W., Wang A., He Q., Tian T., Liu C., Hu L., Shi Y., Liu L., Wang W., Fu Z. Microstructure and mechanical properties of B_4C–TiB_2 ceramic composites prepared via a two-step method. *Journal of the European Ceramic Society*. 2021;41(14):6952–6961. https://doi.org/10.1016/j.jeurceramsoc.2021.07.013
4. Rubink W.S., Ageh V., Lide H., Ley N.A., Young M.L., Casem D.T., Faierson E.J., Scharf T.W. Spark plasma sintering of B_4C and B_4C–TiB_2 composites: Deformation and failure mechanisms under quasistatic and dynamic loading. *Journal of the European Ceramic Society*. 2021;41(6):3321–3332. https://doi.org/10.1016/j.jeurceramsoc.2021.01.044
5. Fahrenholtz W.G., Hilmas G.E. Ultra-high temperature ceramics: Materials for extreme environments. *Scripta Materialia*. 2017;129:94–99. https://doi.org/10.1016/j.scriptamat.2016.10.018
6. Basu B., Raju G.B., Suri A.K. Processing and properties of monolithic TiB_2 based materials. *International Materials Reviews*. 2006;51(6):352–374. https://doi.org/10.1179/174328006X102529
7. Golla B.R., Mukhopadhyay A., Basu B. Review on ultra-high temperature boride ceramics. *Progress in Mmaterials*

Science. 2020;111:100651. https://doi.org/10.1016/j.pmatsci.2020.100651

8. Krutskii Y.L., Bannov A.G., Antonova E.V., Sokolov V.V., Pichugin A.Y., Maksimovskii E.A., Krutskaya T.M., Netskina O.V., Bataev I.A. Synthesis of fine dispersed titanium diboride from nanofibrous carbon. *Ceramics International*. 2017;43(3):3212–3217. https://doi.org/10.1016/j.ceramint.2016.11.146
9. White R.M., Dickey E.C. Mechanical properties and deformation mechanisms of B_4C–TiB_2 eutectic composites. *Journal of the European Ceramic Society*. 2014;34(9): 2043–2050. https://doi.org/10.1016/j.jeurceramsoc.2013.08.012
10. Clayton J.D., Rubink W.S., Ageh V., Choudhuri D., Chen R.R., Du J. Scharf T.W. Deformation and failure mechanics of boron carbide–titanium diboride composites at multiple scales. *JOM: the Journal of the Minerals, Metals & Materials Society*. 2019;71:2567–2575. https://doi.org/10.1007/s11837-019-03548-y
11. Heydari M.S., Baharvandi H.R. Comparing the effects of different sintering methods for ceramics on the physical and mechanical properties of B_4C–TiB_2 nanocomposites. *International Journal of Refractory Metals and Hard Materials*. 2015;51:224–232. https://doi.org/10.1016/j.ijrmhm.2015.04.003
12. Srivatsan T.S., Guruprasad G., Black D., Radhakrishnan R., Sudarshan T.S. Influence of TiB_2 content on microstructure and hardness of TiB_2–B_4C composite. *Powder Technology*. 2005;159(3):161–167. https://doi.org/10.1016/j.powtec.2005.08.003
13. Cai K.F., Nan C.W., Schmuecker M., Mueller E. Microstructure of hot-pressed B_4C–TiB_2 thermoelectric composites. *Journal of Alloys and Compounds*. 2003;350(1-2): 313–318. https://doi.org/10.1016/S0925-8388(02)00993-3
14. Wang A., He Q., Guo W., Liu C., Tian T., Hu L., Liu L., Wang W., Fu Z. Microstructure and properties of hot pressed TiB_2 and SiC reinforced B_4C-based composites. *Materials Today Communications*. 2021;26:102082. https://doi.org/10.1016/j.mtcomm.2021.102082
15. Bogomol .I, Borodianska H., Zhao T., Nishimura T., Sakka Y., Loboda P., Vasylkiv O. a dense and tough (B_4C–TiB_2)–B_4C «composite within a composite» produced by spark plasma sintering. *Scripta Materialia*. 2014;71:17–20. https://doi.org/10.1016/j.scriptamat.2013.09.022
16. Liu Y., Li Z., Peng Y., Huang Y., Huang Z., Zhang D. Effect of sintering temperature and TiB_2 content on the grain size of B_4C–TiB_2 composites. *Materials Today Communications*. 2020;23:100875. https://doi.org/10.1016/j.mtcomm.2019.100875
17. Nikzad L., Orrù R., Licheri R., Cao G. Fabrication and formation mechanism of B_4C–TiB_2 composite by reactive spark plasma sintering using unmilled and mechanically activated reactants. *Journal of the American Ceramic Society*. 2012;95(11):3463–3471. https://doi.org/10.1111/j.1551-2916.2012.05416.x
18. Shestakov V.A., Gudyma T.S., Krutskii Y.L., Uvarov N.F., Brester A.E., Skovorodin I.N. Evaluation of the temperature range suitable for the synthesis of B_4C–TiB_2 and B_4C–ZrB_2 powder composite materials. *Inorganic Materials*. 2021;57:481–486. https://doi.org/10.1134/S0020168521050083

Шестаков В.А., Гудыма Т.С., Крутский Ю.Л., Уваров Н.Ф., Брестер А.Е., Сковородин И.Н. Оценка температурного диапазона процессов синтеза порошковых композиционных материалов B_4C–TIB_2 и B_4C–ZrB_2. *Неорганические материалы*. 2021;57(5):506–511. https://doi.org/10.31857/S0002337X21050080

19. Gudyma T.S., Krutskii Yu.L., Uvarov N.F., Aparnev A.I. Optimization of the obtaining temperature of powder composite material B_4C–ZrB_2 by the boron carbide method. *MATEC Web of Conferences*. 2021;340:5. https://doi.org/10.1051/matecconf/202134001028
20. Krutskii Yu.L., Bannov A.G., Sokolov V.V., Dyukova K.D., Shinkarev V.V., Ukhina A.V., Maksimovskii E.A., Krutskaya T.M., Kuvshinov G.G. Synthesis of highly dispersed boron carbide from nanofibrous carbon. *Nanotechnologies in Russia*. 2013;8:191–198. https://doi.org/10.1134/S1995078013020109

Крутский Ю.Л., Баннов А.Г., Соколов В.В, Дюкова К.Д., Шинкарев В.В., Ухина А.В., Максимовский Е.А., Пичугин А.Ю., Соловьев Е.А., Крутская Т.М., Кувшинов Г.Г. Синтез высокодисперсного карбида бора из нановолокнистого углерода. *Российские нанотехнологии*. 2013;8(3-4):43–48.

21. Kurmashov P.B., Maksimenko V.V., Bannov A.G., Kuvshinov G.G. Horizontal vibrofluidized bed pilot reactor for nanofiber carbon synthesis process. *Khimicheskaya tekhnologiya*. 2013;14(10):635–640. (In Russ.).

Курмашов П.Б., Максименко В.В., Баннов А.Г., Кувшинов Г.Г. Горизонтальный пилотный реактор с виброожиженным слоем для процесса синтеза нановолокнистого углерода. *Химическая технология*. 2013;14(10):635–640.

22. Popov M.V. Improving the efficiency of the process of obtaining a methane-hydrogen mixture by catalytic decomposition of light hydrocarbons: Abstract of the dissertation of PhD. Novosibirsk: NSTU, 2019. 20 p. (In Russ.).

Попов М.В. Повышение эффективности процесса получения метано-водородной смеси каталитическим разложением легких углеводородов: Автореф дис. … канд. техн. наук. Новосибирск: НГТУ, 2019. 20 с.

23. Ordan'yan S.S. Rules for the reactions in B_4C–$Me^{IV–VI}B_2$ systems. *Refractories*. 1993;34:268–271. https://doi.org/10.1007/bf01293229
24. Elyutin V.P., Pavlov Yu.A., Polyakov V.P., Sheboldaev S.B. Interaction of metal oxides with carbon. Moscow: Metallurgiya, 1976. 360 p. (In Russ.).

Елютин В.П., Павлов Ю.А., Поляков В.П., Шеболдаев С.Б. Взаимодействие окислов металлов с углеродом. М.: Металлургия, 1976. 360 с.

25. Niihara K., Morena R, Hasselman D. Evaluation of K_{1c} of brittle solids by the indentation method with low crack-to-indent ratios *Journal of Materials Science Letters*. 1982;1:13–16. https://doi.org/10.1007/BF00724706
26. Blott S.J., Pye K. GRADISTAT: a grain size distribution and statistics package for the analysis of unconsolidated sediments. *Earth Surface Processes and Landforms*. 2001;26(11):1237–1248. https://doi.org/10.1002/esp.261
27. Samsonov G.V. Physical and chemical properties of oxides: Ref. ed. Moscow: Metallurgiya, 1978. 471 p. (In Russ.).

Самсонов Г.В. Физико-химические свойства окислов: Справ. изд. М.: Металлургия, 1978. 471 с.

Information about the Authors

Tat'yana S. Gudyma – Postgraduate Student of the Department of Chemistry and Chemical Technology, Novosibirsk State Technical University (NSTU)
ORCID: 0000-0002-4724-3371
E-mail: gudymatan@mail.ru

Yurii L. Krutskii – Cand. Sci. (Eng.), Associate Professor of the Department of Chemistry and Chemical Technology, NSTU
ORCID: 0000-0003-2524-4143
E-mail: j_krutskii@rambler.ru

Eugene A. Maximovskiy – Cand. Sci. (Chem.), Senior Researcher of the Laboratory of Functional Films and Coatings, Nikolaev Institute of Inorganic Chemistry, Siberian Branch RAS
ORCID: 0000-0002-1555-2719
E-mail: eugene@niic.nsc.ru

Nina Yu. Cherkasova – Cand. Sci. (Eng.), Junior Research of the Research Laboratory of Physicochemical Technologies and Functional Materials, NSTU
ORCID: 0000-0002-5603-7852
E-mail: cherkasova.2013@corp.nstu.ru

Nikita I. Lapekin – Student of the Department of Materials Science in Mechanical Engineering, NSTU
E-mail: lapekin21@mail.ru

Tat'yana V. Larina – Cand. Sci. (Phys.-Math.), Senior Researcher of the Department for Catalytic Studies, Boreskov Institute of Catalysis, Siberian Branch RAS
ORCID: 0000-0002-8020-5270
E-mail: larina@catalysis.ru

Сведения об авторах

Татьяна Сергеевна Гудыма – аспирант кафедры химии и химической технологии, Новосибирский государственный технический университет (НГТУ)
ORCID: 0000-0002-4724-3371
E-mail: gudymatan@mail.ru

Юрий Леонидович Крутский – к.т.н., доцент кафедры химии и химической технологии, НГТУ
ORCID: 0000-0003-2524-4143
E-mail: j_krutskii@rambler.ru

Евгений Анатольевич Максимовский – к.х.н., ст. науч. сотрудник лаборатории функциональных пленок и покрытий, Институт неорганической химии им. А.В. Николаева (ИНХ) СО РАН
ORCID: 0000-0002-1555-2719
E-mail: eugene@niic.nsc.ru

Нина Юрьевна Черкасова – к.т.н., мл. науч. сотрудник научно-исследовательской лаборатории физико-химических технологий и функциональных материалов, НГТУ
ORCID: 0000-0002-5603-7852
E-mail: cherkasova.2013@corp.nstu.ru

Никита Игоревич Лапекин – студент кафедры материаловедения в машиностроении, НГТУ
E-mail: lapekin21@mail.ru

Татьяна Викторовна Ларина – к.ф-м.н., ст. науч. сотрудник отдела исследования катализаторов, Институт катализа им. Г.К. Борескова СО РАН
ORCID: 0000-0002-8020-5270
E-mail: larina@catalysis.ru

Contribution of the Authors

T. S. Gudyma – formation of the main concept, goal and objectives of the study; writing the text, formulation of the conclusions, conducting the calculations, testing the samples

Yu. L. Krutskii – preparation and management of the experiments, provision of the resources.
E. A. Maksimovskiy – conducting the experiments, processing of the research results.
N. Yu. Cherkasova – conducting the calculations, writing the text, testing the samples.
N. I. Lapekin – conducting the calculations, analysis of the research results.
T. V. Larina – scientific guidance, correction of the text and conclusions.

Вклад авторов

Т. С. Гудыма – формирование основной концепции, постановка цели и задачи исследования, подготовка текста, формулировка выводов, проведение расчетов, испытаний образцов, подготовка текста статьи.
Ю. Л. Крутский – подготовка эксперимента, руководство проведением эксперимента, обеспечение ресурсами.
Е. А. Максимовский – проведение экспериментов, обработка результатов исследований.
Н. Ю. Черкасова – проведение расчетов, испытаний образцов, подготовка текста статьи.
Н. И. Лапекин – проведение расчетов, анализ результатов исследований.
Т. В. Ларина – научное руководство, корректировка текста, корректировка выводов.

Received 14.06.2022
Revised 13.10.2022
Accepted 17.10.2022

Статья поступила 14.06.2022 г.
Доработана 13.10.2022 г.
Принята к публикации 17.10.2022 г.